



## Resistance to H<sub>2</sub>O<sub>2</sub>-induced oxidative stress in human cells of different phenotypes

Valeriy Zenin<sup>a</sup>, Julia Ivanova<sup>a</sup>, Natalia Pugovkina<sup>a</sup>, Alla Shatrova<sup>a</sup>, Nikolay Aksenov<sup>a</sup>, Irina Tyuryaeva<sup>a</sup>, Kseniya Kirpichnikova<sup>a</sup>, Ivan Kuneev<sup>a,b</sup>, Andrei Zhuravlev<sup>a,c</sup>, Ekaterina Osyayeva<sup>a,c</sup>, Ekaterina Lyublinskaya<sup>a,b</sup>, Ilyuza Gazizova<sup>a,b</sup>, Nikita Guriev<sup>a,b</sup>, Olga Lyublinskaya<sup>a,\*</sup>

<sup>a</sup> Department of Intracellular Signaling and Transport, Institute of Cytology, Russian Academy of Sciences, Tikhoretskii pr. 4, St. Petersburg, 194064, Russia

<sup>b</sup> Peter the Great St. Petersburg Polytechnic University, Polytechnicheskaya st. 29, St. Petersburg, 195251, Russia

<sup>c</sup> Faculty of Biology, St. Petersburg State University, 7/9 Universitetskaya Emb., St. Petersburg, 199034, Russia

### ARTICLE INFO

#### Keywords:

Hydrogen peroxide  
H<sub>2</sub>O<sub>2</sub>  
Genetically encoded biosensors  
HyPer  
Kinetics  
Rate constants  
H<sub>2</sub>O<sub>2</sub> gradient  
Induced pluripotent stem cells  
Mesenchymal stem/stromal cells  
Cell reprogramming

### ABSTRACT

Application of genetically encoded biosensors of redox-active compounds promotes the elaboration of new methods for investigation of intracellular redox activities. Previously, we have developed a method to measure quantitatively the intracellular concentration of hydrogen peroxide (H<sub>2</sub>O<sub>2</sub>) in living cells using genetically encoded biosensor HyPer. In the present study, we refined the method and applied it for comparing the antioxidant system potency in human cells of different phenotypes by measuring the gradient between the extracellular and cytoplasmic H<sub>2</sub>O<sub>2</sub> concentrations under conditions of H<sub>2</sub>O<sub>2</sub>-induced external oxidative stress. The measurements were performed using cancer cell lines (K-562 and HeLa), as well as normal human cells – all expressing HyPer in the cell cytoplasm. As normal cells, we used three isogenic lines of different phenotypes – mesenchymal stem/stromal cells (MSCs), induced pluripotent stem cells (iPSCs) derived from MSCs by reprogramming, and differentiated iPSC progenies with the phenotype resembling precursory MSCs. When exposing cells to exogenous H<sub>2</sub>O<sub>2</sub>, we showed that at low oxidative loads (<50 μM of H<sub>2</sub>O<sub>2</sub>) the gradient depended on extracellular H<sub>2</sub>O<sub>2</sub> concentration. At high loads (>50 μM of H<sub>2</sub>O<sub>2</sub>), which caused the exhaustion of thioredoxin activity in the cell cytoplasm, the gradient stabilized, pointing out that it is the functional status of the thioredoxin-dependent enzymatic system that drives the dependence of the H<sub>2</sub>O<sub>2</sub> gradient on the oxidative load in human cells. At high H<sub>2</sub>O<sub>2</sub> concentrations, the cytoplasmic H<sub>2</sub>O<sub>2</sub> level in cancer cells was found to be several hundred times lower than the extracellular one. At the same time, in normal cells, extracellular-to-intracellular gradient amounted to thousands of times. Upon reprogramming, the potency of cellular antioxidant defense increased. In contrast, differentiation of iPSCs did not result in the changes in antioxidant system activity in the cell cytoplasm, assuming that intensification of the H<sub>2</sub>O<sub>2</sub>-detoxification processes is inherent to a period of early human development.

### 1. Introduction

Hydrogen peroxide (H<sub>2</sub>O<sub>2</sub>), being a product of oxygen metabolism, is generated in all cells of aerobic organisms and participates in various metabolic and signaling cascades [1–3]. The maintenance of physiological H<sub>2</sub>O<sub>2</sub> intracellular concentration is crucial for cell functioning and viability. Stressful imbalance caused by the elevation of

intracellular level of H<sub>2</sub>O<sub>2</sub> over the basal one, which is strictly controlled by cellular redox systems, is classified as ‘oxidative stress’ or, more specifically, ‘oxidative distress’ (the latter is opposed to ‘oxidative eustress’ – an elevation in H<sub>2</sub>O<sub>2</sub> level arising from the physiological needs) [3,4]. The excessive accumulation of intracellular H<sub>2</sub>O<sub>2</sub> can occur due to internal pathological processes and external factors disturbing cellular redox metabolism, as well as due to an increase of H<sub>2</sub>O<sub>2</sub>

**Abbreviations:** cpYFP, circularly permuted yellow fluorescent protein; DTT, dithiothreitol; MSCs, mesenchymal stem/stromal cells; iPSCs, induced pluripotent stem cells; iPSC-MSCs, MSC-like differentiated descendants of iPSCs.

\* Corresponding author.

E-mail address: [olga.lyublinskaya@incras.ru](mailto:olga.lyublinskaya@incras.ru) (O. Lyublinskaya).

<https://doi.org/10.1016/j.redox.2022.102245>

Received 2 December 2021; Received in revised form 14 January 2022; Accepted 19 January 2022

Available online 26 January 2022

2213-2317/© 2022 The Authors.

Published by Elsevier B.V. This is an open access article under the CC BY-NC-ND license

(<http://creativecommons.org/licenses/by-nc-nd/4.0/>).

flow from the outside of a cell. The increase of extracellular  $H_2O_2$  level can, in turn, arise from environmental stresses (such as radiation, tobacco smoke, toxicants, etc.), activity of the immune system, or due to metabolic disorders in surrounding tissues [4,5].

Under conditions of externally induced oxidative stress, the antioxidant defense system, which includes cellular enzymes responsible for  $H_2O_2$  elimination (peroxiredoxins, glutathione peroxidases, catalase) and reduction of oxidized proteins (thioredoxins and glutaredoxins), counteracts the damaging effects of stress. The finite rate of penetration of  $H_2O_2$  through plasma membrane and its effective intracellular elimination result in the emergence of  $H_2O_2$  concentration gradient – the level of  $H_2O_2$  inside a cell appears to be much lower than that outside [6–8]. The value of the extracellular-to-intracellular  $H_2O_2$  gradient can be therefore considered as a measure of antioxidative activity in cells. A first theoretical assessment of the gradient in oxidatively stressed human cells was made by Antunes and Cadenas in 2000 [6]. The results of the analysis performed showed that, if  $H_2O_2$  is constantly present outside the cells, the established intracellular concentration of  $H_2O_2$  can be ten-fold lower in comparison to extracellular. Later, considering the contribution of such effective  $H_2O_2$ -detoxifying enzymes as peroxiredoxins, it became clear that the gradient can be much higher – about several hundred [8], and that it is established very quickly – during the first milliseconds after the stress induction [9]. Most recent findings showed that this gradient can vary, being dependent on the oxidative load on a cell [10]. At high  $H_2O_2$  doses, the oxidation/reduction cycle of peroxiredoxins can collapse due to their hyperoxidation [11] that causes the drop in  $H_2O_2$ -detoxification capacity in a cell. Consequently, the extracellular-to-intracellular  $H_2O_2$  gradients are low at high oxidative loads and high at low ones. It was found that in yeast the  $H_2O_2$  gradient, which is established at a high oxidative load, is several tens, and at low – about several hundred [10]. To what extent the  $H_2O_2$  gradient in human cells can vary is still not clear.

Recently, we have shown that intracellular concentration of  $H_2O_2$  can be measured using HyPer, a genetically encoded  $H_2O_2$  biosensor [12]. HyPer is a chimeric protein [13] composed from the permuted yellow fluorescent protein (cpYFP) and  $H_2O_2$ -sensitive domain of the bacterial transcription factor OxyR, which is responsible for sensing  $H_2O_2$  in *E.coli* [14]. Upon HyPer exposure to  $H_2O_2$ , the OxyR domain undergoes conformational changes which influence the protonation of tyrosine residues in cpYFP that, in turn, leads to changes in its fluorescence [15]. In our previous study [12], we have demonstrated that in  $H_2O_2$ -exposed cells, intracellular  $H_2O_2$  concentration can be derived from the analysis of kinetics of HyPer oxidation, monitored with the use of flow cytometry. Performing such measurements in the model cells (human erythroleukemia K-562 cells, resuspended in phosphate-buffered saline), we found that the gradient between the extracellular and cytoplasmic  $H_2O_2$  concentrations is about 400-fold under micromolar extracellular  $H_2O_2$  loads. In the present study, we refined the method presented earlier, aiming to achieve a more accurate estimation of  $H_2O_2$  gradients in oxidatively stressed cells resuspended in a standard growth medium. The improved method allows to measure the extracellular-to-intracellular  $H_2O_2$  gradients and evaluate the potency of antioxidant defense system in cells of different phenotypes at various oxidative loads. Using this method, we compared  $H_2O_2$ -detoxifying activity in the cytoplasm of human cancer cell lines (K-562 and HeLa), mesenchymal stem/stromal cells (MSCs), induced pluripotent stem cells (iPSCs) derived from MSCs by reprogramming, and differentiated progenies of iPSCs with the phenotype resembling precursory MSCs (iPSC-MSCs).

## 2. Materials and methods

### 2.1. Cell cultures

**K-562 cells.** Human K-562 erythroleukemia cells (Russian Cell Culture Collection, Institute of Cytology, St.Petersburg, Russia) were

transduced [16] with lentiviral vectors (Evrogen Ltd, Moscow, Russia) encoding HyPer-cyto or SypHer-cyto proteins. SypHer is a redox-inactive modification of cpYFP-OxyR protein, which is commonly used as an optimum control molecule for HyPer [15]. K-562 cells were cultured in RPMI medium (Biotech Ltd, Russia) supplemented with 10% fetal bovine serum (FBS) (HyClone, USA), 1% L-glutamine, and 1% penicillin-streptomycin. Cells were maintained at 37 °C, 5%  $CO_2$ , and were passaged twice a week at the split ratio of 1:4.

**HeLa cells.** HeLa (cervix carcinoma) cells (Russian Cell Culture Collection, Institute of Cytology, St.Petersburg, Russia) were transduced with a lentiviral vector encoding HyPer-cyto (Evrogen Ltd, Moscow, Russia) using the protocol described previously [16]. Cells were cultivated in DMEM/F12 medium (Gibco, USA) supplemented with 10% FBS (HyClone, USA), 1% L-glutamine, and 1% penicillin-streptomycin at 37 °C, 5%  $CO_2$ . Cells were subcultured twice a week at the split ratio of 1:5.

**Mesenchymal stem/stromal cells (MSCs).** Human mesenchymal stem/stromal cells were isolated from a desquamated endometrium of menstrual blood from a healthy donor (line#2804 [17]). Cells exhibited properties typical of mesenchymal stem/stromal cell cultures: fibroblast-like morphology, multipotency, and expression of standard surface markers [18]. MSCs were cultivated in DMEM/F12 medium (Gibco, USA) supplemented with 10% FBS (HyClone, USA), 1% L-glutamine, and 1% penicillin-streptomycin. Cells were maintained at 37 °C, 5%  $CO_2$ , and were subcultured twice a week at the split ratio of 1:3. At the 6th passage, MSCs were transduced [16] with the lentiviral vector encoding HyPer-cyto (Evrogen Ltd, Moscow, Russia). In the experiments, cells cultivated for up to 15 passages were used.

**Induced pluripotent stem cells (iPSCs).** iPSCs were derived from MSCs expressing HyPer in the cell cytoplasm using CytoTune-iPS 2.0 Sendai Reprogramming Kit according to manufacturer's instruction. iPSCs obtained possess clonal growth morphology, a diploid karyotype, express pluripotency markers Oct-4, NANOG, SSEA-4, SOX2, alkaline phosphatase, and are able to differentiate into cell types of three germ layers (see Results section). Cells were cultivated at 37 °C and normoxia (21%  $O_2$ ) with 5%  $CO_2$  content on Matrigel-coated (Corning, USA) dishes in mTeSR medium (STEMCELL Technologies, Canada) and subcultured mechanically once a week.

**Differentiated iPSC progenies (iPSC-MSCs).** iPSCs, which constantly express HyPer-cyto, were spontaneously differentiated through embryoid bodies (EB) formation. iPSC colonies were cut into pieces and plated into non-adhesive plastic dishes in the Knockout DMEM/F12 (Gibco, USA) medium supplemented with 20% serum replacement, 1% non-essential amino acids (Sigma, USA), 0.1 mM  $\beta$ -mercaptoethanol (Merck, USA), 1% penicillin-streptomycin. Within one week, cystic EB were formed. After that, EB were transferred into the adhesive tissue culture dishes and cultivated in DMEM/F12 medium (Gibco, USA) with 10% FBS (HyClone, USA), 1% L-glutamine, and 1% penicillin-streptomycin. Spontaneously differentiated cells derived from the attached EB were subcultured once a week at the split ratio 1:3. After 2–3 passages, the culture was composed of morphologically homogeneous fibroblast-like HyPer-expressing cells which were positive for the mesenchymal marker vimentin. We characterized these cells and revealed that their phenotype was similar to that of parental MSCs. Cells were positive for CD 90, CD 105, CD 73, CD 44, CD 140b marker expression, negative for HLA DR, and possessed typical for MSCs ability to differentiate into osteoblasts and adipocytes (see Results section). Basing on the minimal criteria for defining multipotent mesenchymal stem/stromal cells formulated by the International Society for Cellular Therapy [18], we classified differentiated progenies of iPSCs as MSCs and named them iPSC-MSCs.

### 2.2. $H_2O_2$ -induced oxidative stress

To investigate the ability of cells to counteract oxidative stress, both short-term (10-min) and long-term (24-h) incubations with  $H_2O_2$  have

been exploited. K-562, HeLa, MSCs, and iPSC-MSCs were seeded in 3 cm dishes or 24-well plates overnight before the experiments (25,000 cells per 1 mL of medium). iPSCs were seeded at arbitrary cell density in 24-well plates 3 days before the exposure to H<sub>2</sub>O<sub>2</sub>.

Short-term (10-min) exposure to H<sub>2</sub>O<sub>2</sub> was used for the analysis of HyPer oxidation immediately after the oxidative stress induction. In these experiments, prior to H<sub>2</sub>O<sub>2</sub> exposure, adherent cells (HeLa, MSCs, iPSCs, iPSC-MSCs) were harvested with 0.05% trypsin-EDTA solution. After that, these cells, as well as suspension K-562 cells, were resuspended in the fresh DMEM/F12 medium (supplemented with FBS and L-glutamine) at the density of 25,000 cells/mL. Cell samples were aliquoted in the flow cytometry tubes (600 µL per tube) and incubated at standard growth conditions for 20 min to provide adaptation of cells to the new environment. After that, H<sub>2</sub>O<sub>2</sub> at concentrations ranged from 2 to 100 µM was added to the tubes and cell samples were immediately analyzed with CytoFLEX flow cytometer (Beckman Coulter, USA). High dilution of cell suspensions provided near steady-state conditions of the oxidative load. At cell density used, the drop of extracellular H<sub>2</sub>O<sub>2</sub> concentration due to the peroxide scavenging by cells was negligible during the first 10 min after H<sub>2</sub>O<sub>2</sub> addition [12]. In the experiments on thioredoxin system inhibition, before harvesting, cells were pre-incubated for 3 h with the auranofin, thioredoxin reductase inhibitor, at standard growth conditions at a concentration of 100 nM. Auranofin was also added to the fresh medium used for cell harvesting and resuspension.

Long-term (24-h) expositions were used to assess the damaging effects of H<sub>2</sub>O<sub>2</sub> concentrations applied. Prior to H<sub>2</sub>O<sub>2</sub> exposure, cells in several dishes (wells) were counted to calculate the doses of H<sub>2</sub>O<sub>2</sub> added. Doses were quantified on the mole-per-cell basis [19] by the normalization of the added H<sub>2</sub>O<sub>2</sub> molar quantity to the number of cells in the dish (well). In the rest of the dishes (wells) growth medium was changed to the fresh DMEM/F12 medium supplemented with FBS and L-glutamine. H<sub>2</sub>O<sub>2</sub> was added to cells at concentrations ranging from 2 to 800 µM (corresponding doses 0.08–14 pmol/cell) and was incubated for 24 h. After that, cell viability was evaluated with the use of flow cytometry.

### 2.3. Monitoring of HyPer oxidation kinetics

Kinetics of HyPer oxidation was monitored with CytoFLEX flow cytometer (Beckman Coulter, USA). Analysis lasted for 10 min after H<sub>2</sub>O<sub>2</sub> addition. During the analysis, a mixture of air and CO<sub>2</sub> (5%) was supplied into the sample tube to stabilize physiological pH in the cell medium. Constant CO<sub>2</sub> pumping made it possible to prevent variations in the HyPer signal arising from the alkalization of the cell medium, which is usually detected during long-term measurements in atmospheric air. In the cell cultures used for experiments, the fraction of HyPer-expressing cells was about 90–95%. HyPer fluorescence in gated HyPer-positive cells was examined by monitoring fluorescence signal at 525 nm registered at 488 nm excitation (hereafter denoted as *FL<sub>blue</sub>* signal), which reflects the accumulation of oxidized form of sensor [16]. Similarly, the signal measured at 525 nm under 405 nm excitation (hereafter denoted as *FL<sub>violet</sub>* signal) was used to monitor the accumulation of the reduced sensor.

For the calibration of HyPer signals (described in the Results section), *FL<sub>blue</sub>* and *FL<sub>violet</sub>* were also measured in the cells pretreated with the high doses of dithiothreitol (DTT, 30 mM, 10 min) and H<sub>2</sub>O<sub>2</sub> (0.5 mM, 5 min) to achieve a total HyPer reduction and oxidation, respectively. Cell pretreatments were performed at standard growth conditions (37 °C and 5% of CO<sub>2</sub>) in flow cytometry tubes.

### 2.4. Calculation of gradient between the extracellular and intracellular H<sub>2</sub>O<sub>2</sub> concentrations

To measure the extracellular-to-intracellular H<sub>2</sub>O<sub>2</sub> concentration gradient in cells exposed to exogenous H<sub>2</sub>O<sub>2</sub> we used equations derived

by Brito and Antunes [20]. According to these equations, upon the oxidative stress induction, the fraction of reduced HyPer begins to fall and, under the permanent external oxidative load, reaches with time the steady-state level due to the concurrent processes of sensor oxidation and reduction. In the case of full HyPer reduction at the initial moment of time, the kinetics of HyPer oxidation is described as follows [12]:

$$HyPer_{rd}(t) = HyPer_{rd\ ss} + e^{-(k_{ox}+k_{rd}) \times t} \times (1 - HyPer_{rd\ ss}) \quad (1)$$

$$HyPer_{rd\ ss} = \frac{k_{rd}}{k_{rd} + k_{ox}} \quad (2)$$

In these equations, *HyPer<sub>rd</sub>(t)* refers to the fraction of HyPer in the reduced form observed in a cell at time *t*. *HyPer<sub>rd\ ss</sub>* is the steady-state level of the reduced HyPer fraction established with time. *k<sub>ox</sub>* and *k<sub>rd</sub>* are apparent first-order rate constants for the oxidation and reduction of HyPer (corresponding to *k<sub>activation</sub>* and *k<sub>switch-off</sub>* in Ref. [20]), respectively. *k<sub>rd</sub>* depends on the activity of thiol-disulfide exchange systems of the cells. *k<sub>ox</sub>* depends on the intracellular level of H<sub>2</sub>O<sub>2</sub> [20]:

$$k_{ox} = k_{HyPer+H2O2} \times [H_2O_2]_{in} \quad (3)$$

where *[H<sub>2</sub>O<sub>2</sub>]<sub>in</sub>* is an intracellular peroxide concentration averaged over the sites of HyPer localization (in this study it is a cell cytosol), and *k<sub>HyPer+H2O2</sub>* = 5 × 10<sup>5</sup> M<sup>-1</sup>s<sup>-1</sup> is the second-order rate constant for the reaction between HyPer and hydrogen peroxide (known from the previously published studies [21]).

Under conditions of high oxidative loads, which result in the full HyPer oxidation (*HyPer<sub>rd\ ss</sub>* → 0), *k<sub>rd</sub>* << *k<sub>ox</sub>*, according to Eq. (2), and the kinetics of HyPer oxidation is described by simple exponential dependence (Eq. 12 [20]):

$$HyPer_{rd}(t) = e^{-(k_{ox}) \times t} \quad (4)$$

Eqs. (1) and (4), upon linearization, are transformed into the following dependencies (Eqs. (8) and (16) [20]):

$$\ln \left[ \frac{HyPer_{rd}(t) - HyPer_{rd\ ss}}{1 - HyPer_{rd\ ss}} \right] = -(k_{ox} + k_{rd}) \times t \quad (5)$$

$$\ln[HyPer_{rd}(t)] = -(k_{ox}) \times t \quad (6)$$

In the present study, measuring the dependence *HyPer<sub>rd</sub>(t)* after the oxidative stress induction and fitting it with Eq. (1), we determined *k<sub>rd</sub>*, *k<sub>ox</sub>*, as well as *[H<sub>2</sub>O<sub>2</sub>]<sub>in</sub>* (Eq. (3)). Using the value of *[H<sub>2</sub>O<sub>2</sub>]<sub>in</sub>* and concentration of exogenous H<sub>2</sub>O<sub>2</sub> added to cell suspension *[H<sub>2</sub>O<sub>2</sub>]<sub>ex</sub>*, we calculated the extracellular-to-intracellular H<sub>2</sub>O<sub>2</sub> gradient:

$$\text{gradient} = [H_2O_2]_{ex} / [H_2O_2]_{in} \quad (7)$$

By measuring H<sub>2</sub>O<sub>2</sub> gradients in cells of different phenotypes, we compare the potency of cell antioxidant systems.

### 2.5. Cell viability

To assess H<sub>2</sub>O<sub>2</sub> toxic effect, cells were exposed to H<sub>2</sub>O<sub>2</sub> at various concentrations for 24 h. Cell viability was estimated by flow cytometry (CytoFLEX flow cytometer, Beckman Coulter, USA; 488 nm laser) using propidium iodide staining (50 µg/mL).

### 2.6. Immunofluorescence

Cells grown on coverslips were fixed with 4% formalin in phosphate-buffered saline (PBS), permeabilized with 0.1% Triton X-100, incubated with 1% bovine serum albumin for 40 min to block non-specific binding, treated with the primary antibodies for 1 h, washed with PBS/0.1% Tween-20, treated with secondary antibodies for 1 h, washed with PBS/0.1% Tween-20 and counterstained with 1 µg/mL DAPI. The coverslips were mounted in 2% propyl gallate and visualized using a confocal microscope (Olympus FV3000, Olympus Corporation). Primary

antibodies: anti-Oct-4 (C-10) (Santa Cruz Biotechnology, USA), anti-NANOG (Invitrogen, USA), anti-SOX-2 (Millipore, USA), anti-SSEA-4 (Millipore, USA), anti-Vimentin (BD Pharmingen, USA), all in dilution 1:100.

## 2.7. Cell phenotyping

Cells were harvested with 0.05% trypsin-EDTA solution, washed, suspended in PBS supplemented with 2% FBS, incubated with antibodies to phycoerythrin-conjugated antibodies CD 90, CD 105, CD 73, CD, 140b, HLA DR (all from BD Pharmingen), CD 44 (eBioscience, USA) for 30 min in flow cytometry tubes at room temperature in the dark following the manufacturer instructions, and analyzed using CytoFLEX flow cytometer (Beckman Coulter, USA; 561 nm laser).

## 2.8. Statistics

All experiments were repeated at least 3 times. Data are presented as means  $\pm$  SD, when indicated. Statistical significance in the pairwise comparisons was evaluated by *t*-test, and  $p < 0.05$  was considered to be significant. Flow cytometry histograms and microscopy images shown in the paper correspond to the most representative experiments.

## 3. Results

Our previous study [12] showed that upon exposure of HyPer-expressing cells to exogenous  $H_2O_2$ , its intracellular concentration can be estimated quantitatively by analyzing HyPer oxidation kinetics just after the addition of  $H_2O_2$  to the cell suspension. To monitor the oxidation kinetics, we measured HyPer fluorescence signals by flow cytometry at different time points after the oxidative stress induction and then derived the percentages of oxidized/reduced sensor from these measurements. In the present study, we developed a method that allows real-time tracking of HyPer fluorescence which afterward can be directly converted to the kinetic curves. To elaborate the method, we used human erythroleukemia K-562 cells stably expressing HyPer in the cell

cytoplasm (Supplemental Fig. S1).

### 3.1. Elaboration of a method for real-time monitoring of HyPer oxidation

HyPer has two excitation maxima at 420 and 500 nm and emits intense green fluorescence peaked at 516 nm. Upon oxidation of HyPer, the intensity of fluorescence excited at 420 nm ( $FL_{violet}$ ) decreases, while the fluorescence excited at 500 nm ( $FL_{blue}$ ) proportionally increases. Due to this, it is possible to monitor the ratio between the oxidized and reduced forms of HyPer upon the induction of oxidative stress in real time by recording the time-dependent changes in the fluorescence signals. Indeed, in our experiments, the addition of exogenous  $H_2O_2$  to K-562 cells led to the immediate gradual increase of  $FL_{blue}$  signal with simultaneous decrease of the  $FL_{violet}$  signal, associated with the accumulation of oxidized and exhaustion of the reduced forms of HyPer, respectively (Fig. 1A). In the case of arbitrary device settings, the increase in  $FL_{blue}$  signal is not equal to the decrease in  $FL_{violet}$ . However, by varying the voltage or gain settings for the cytometer detectors, the changes in fluorescence signals can be aligned (Fig. 1A). Under these conditions, the sum signal from the oxidized and reduced form of HyPer ( $FL_{blue} + FL_{violet}$ ) does not depend on the redox status of the sensor and represents only the overall amount of HyPer protein in the cell cytoplasm. Consequently, the normalization of each signal ( $FL_{blue}$  or  $FL_{violet}$ ) to the sum signal allows reducing the level of noise, which results, to a great extent, from various HyPer expression levels in cells (Fig. 1B). That kind of signal processing enables the improvement of the accuracy of the kinetic measurements.

In the next step, we calibrated the normalized HyPer signals in K-562 cells using high concentrations of  $H_2O_2$  and DTT providing the total oxidation and total reduction of the sensor, respectively. We found that a saturative dose of  $H_2O_2$  (0.5 mM, 5 min) resulted in the full oxidation of HyPer, whereas the addition of various concentrations of DTT (up to 30 mM) did not lead to the significant changes of HyPer fluorescence signals, which indicates the fully reduced status of HyPer in the cell cytoplasm under physiological conditions. The calibration allowed linking the HyPer fluorescence signal and the fraction of reduced sensor in the

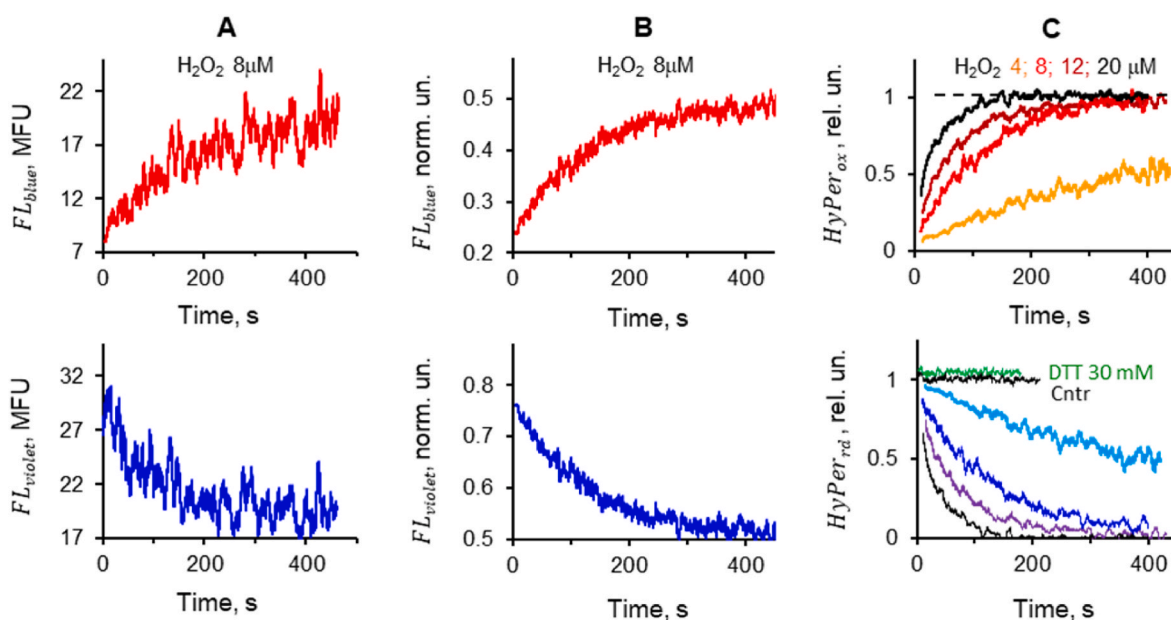


**Fig. 1. Real-time monitoring of HyPer oxidation in K562 cells.** (A–B) Increase of the HyPer  $FL_{blue}$  fluorescence signal and simultaneous decrease of the  $FL_{violet}$  signal registered after the addition of  $H_2O_2$  (8  $\mu$ M) to cell suspension; (A) – raw data, (B) – signals normalized to the total signal ( $FL_{blue} + FL_{violet}$ ); normalization significantly reduces the signal noise; dynamics of fluorescence signals reflects the accumulation of oxidized and exhaustion of reduced forms of HyPer followed after  $H_2O_2$  addition. (C) Oxidized and reduced HyPer fractions in the control (untreated) K562 cells, cells exposed to DTT (30 mM, 10 min), as well as kinetic curves depicting HyPer oxidation after addition of different concentrations of  $H_2O_2$ . Abbreviations:  $FL_{blue}$ , EX488/FL525 signal;  $FL_{violet}$ , EX405/FL525 signal; MFU, mean fluorescence units;  $HyPer_{red}$ , reduced HyPer fraction;  $HyPer_{ox}$ , oxidized HyPer fraction; DTT, dithiothreitol; Cntr, control (untreated) cells.



cell cytoplasm  $HyPer_{rd}$ :

$$HyPer_{rd} = \frac{FL_{violet} - FL_{min}}{FL_{max} - FL_{min}} \quad (8)$$

where  $FL_{violet}$  is a normalized signal measured in the cells of interest at violet laser excitation, and  $FL_{max}$  and  $FL_{min}$  are normalized signals measured in untreated cells and cells treated with the saturative dose of  $H_2O_2$ , respectively. Using Eq. (8), we finally obtained the kinetic curves which described the oxidation of sensor at various oxidative loads (Fig. 1C).

In addition, since HyPer is a pH-dependent sensor, to ensure that  $HyPer_{rd}$  measurements are not influenced by pH variations under the experimental conditions used, a set of experiments with K-562 cells constantly expressing SypHer-cyto, redox-inactive modification of cpYFP-OxyR protein (an optimum control molecule for HyPer that exhibits identical fluorescence properties, pH sensitivity, intracellular localization, etc. [15]), have been performed. SypHer-expressing cells did not respond to  $H_2O_2$  treatments (2–50  $\mu M$ ) (see Supplement, Fig. S2), giving confidence in the reliability of kinetic HyPer-based measurements.

Thus, at the first step of experiments, we worked out the method that allows real-time monitoring of the reduced HyPer fraction  $HyPer_{rd}$  upon exposure of cells to exogenous  $H_2O_2$  (Fig. 1C).

### 3.2. Measurement of the extracellular-to-intracellular $H_2O_2$ gradient

Next, we analyzed the kinetics of HyPer oxidation upon the oxidative stress induction in K-562 cells. We confirmed that the dependence of reduced HyPer fraction on time is described by Eq. (1) (Methods Section) and can be linearized in the logarithmic scale, in accordance with Eqs. (5) and (6) (Fig. 2A). Fitting the kinetic curves with Eq. (1) allowed us to assess  $[H_2O_2]_{in}$  and then calculate the gradient between the extracellular and cytoplasmic concentration of  $H_2O_2$  established at different oxidative loads (Table 1). At low  $H_2O_2$  concentrations, the

gradient was close to  $10^3$  and tended to decrease with increasing loads. In contrast, at high concentrations, which caused full HyPer oxidation, the gradient did not depend on added  $H_2O_2$  concentration (Fig. 2B) and was equal to  $440 \pm 20$ . Importantly, the same gradient value was observed at any oxidative load in cells with the diminished thioredoxin activity (preincubated with thioredoxin reductase inhibitor auranofin), pointing out that the gradient stabilization at high oxidative loads is associated with the saturation of thioredoxin-dependent enzymatic activity, presumably, activity of peroxiredoxins (Fig. 2B).

To check whether the  $H_2O_2$  concentrations used were cytotoxic, we assessed the viability of K-562 cells on the next day after the stress induction. 24-hour incubation with  $H_2O_2$  at concentrations equal or lower than 8  $\mu M$  did not cause cytotoxic effect, while 25  $\mu M$  (which matches the dose of 1 pmol/cell) led to 50% cell death and 50  $\mu M$  (2 pmol/cell) was almost completely lethal (Fig. 2C).

Then, we checked the impact of HyPer expression on the cell response to  $H_2O_2$ -induced stress. First, we evaluated the proportion of HyPer-positive and negative cells in K-562 populations that survived the stress and found no difference with the control (nontreated) samples (Fig. 2C). Further, we analyzed the kinetics of HyPer oxidation in cells with the different expression levels of the sensor. Using gating technique (for details see Supplement, Fig. S3), we chose for analysis cell populations with the same average cell size (based on the forward scattering signal) but differed in the average fluorescence intensity ( $FL_{blue} + FL_{violet}$ ) by 6 times. Again, no difference in  $H_2O_2$  gradients was found between these populations (Fig. 2D).

Thus, we showed that under conditions of external steady-state  $H_2O_2$ -induced stress, our method enables accurately evaluating the extracellular-to-intracellular gradient of  $H_2O_2$  concentration.

### 3.3. Resistance to $H_2O_2$ -induced stress of cells with different phenotypes

In the last part of the study, in order to compare the potency of antioxidant defense systems of different cells, we evaluated the  $H_2O_2$

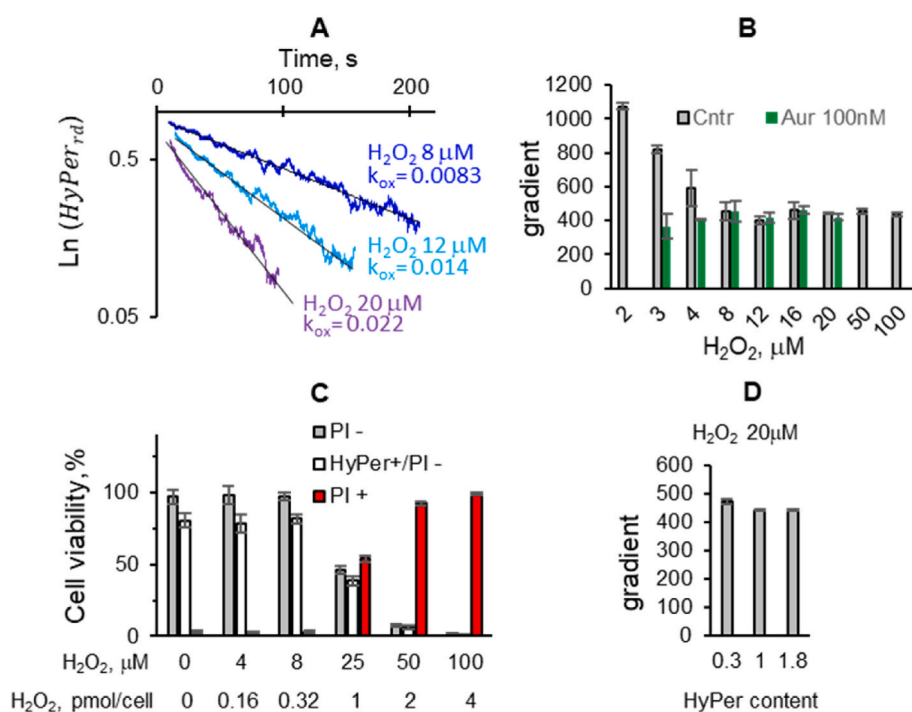


**Fig. 2.** Measurement of the peroxide gradient in K-562 cells exposed to different concentrations of  $H_2O_2$ . (A) Linearization of the kinetic curves for the reduced HyPer fraction drop after  $H_2O_2$  addition to cell suspension; the slope represents the sensor oxidation rate constant (Eq. (6), Methods section). (B) Gradients between the extracellular and cytoplasmic peroxide concentrations in the control cells and cells preincubated with the thioredoxin reductase inhibitor auranofin measured at different  $H_2O_2$  loads (calculated using Eq. (7), Methods section). (C) Total (PI-) and HyPer-positive (HyPer+/PI-) populations of viable K-562 cells, as well as non-viable (PI+) cell fractions, revealed after 24-h exposure to different concentrations of  $H_2O_2$  (corresponding  $H_2O_2$  doses are shown below the axis). (D) Gradients between the extracellular (20  $\mu M$ ) and cytoplasmic peroxide concentrations at different levels of HyPer expression in cells; in each cell sample ( $N = 3$ ), cell populations with low and high HyPer expression were selected by gating (see Supplement Fig. S3), HyPer content in these populations was assessed by normalizing the mean total fluorescence signal ( $FL_{blue} + FL_{violet}$ ) in gated cells to the mean total signal in ungated HyPer-positive cells in this sample. Data (B–D) are shown as mean  $\pm$  SD ( $N > 3$ ). Abbreviations:  $HyPer_{rd}$ , reduced HyPer fraction;  $k_{ox}$ , rate constant of HyPer oxidation; Cntr, control cells (untreated with auranofin); Aur, auranofin-treated cells; PI-, propidium iodide-negative (viable) cells; PI+, propidium iodide-positive (non-viable) cells; HyPer+/PI-, HyPer-positive viable cells;  $FL_{blue}$ , EX488/FL525 signal;  $FL_{violet}$ , EX405/FL525 signal.

**Table 1**

Intracellular  $\text{H}_2\text{O}_2$  levels,  $\text{H}_2\text{O}_2$  gradients, as well as rate constants of HyPer oxidation, derived from the analysis of HyPer oxidation kinetics in  $\text{H}_2\text{O}_2$ -exposed K562 cells.

Parameters	Extracellular hydrogen peroxide concentration $[\text{H}_2\text{O}_2]_{\text{ex}}$							
	3 $\mu\text{M}$	4 $\mu\text{M}$	8 $\mu\text{M}$	12 $\mu\text{M}$	16 $\mu\text{M}$	20 $\mu\text{M}$	50 $\mu\text{M}$	100 $\mu\text{M}$
$k_{\text{ox}}$ , $\text{s}^{-1}$ ( $N > 3$ )	$(18 \pm 1) \times 10^{-4}$	$(30 \pm 1) \times 10^{-4}$	$(9 \pm 1) \times 10^{-3}$	$(16 \pm 1) \times 10^{-3}$	$(18 \pm 3) \times 10^{-3}$	$(22.5 \pm 0.3) \times 10^{-3}$	$(55 \pm 1) \times 10^{-3}$	$(116 \pm 3) \times 10^{-3}$
$\text{HyPer}_{\text{rd ss}}$ , %	$36 \pm 3$	$27 \pm 9$	$3 \pm 1$	$2 \pm 1$	$1 \pm 0.7$	0	0	0
$[\text{H}_2\text{O}_2]_{\text{in}}$ , nM	$3.7 \pm 0.1$	$6 \pm 1$	$18 \pm 2$	$30 \pm 2$	$35 \pm 5$	$45.5 \pm 0.5$	$110 \pm 3$	$231 \pm 6$
gradient	$820 \pm 20$	$600 \pm 100$	$450 \pm 50$	$400 \pm 20$	$460 \pm 50$	$441 \pm 5$	$450 \pm 10$	$430 \pm 10$

**Abbreviations:**  $k_{\text{ox}}$ , apparent first-order rate constant of HyPer oxidation; *gradient*, ratio between the extracellular and intracellular (cytoplasmic) peroxide concentration;  $[\text{H}_2\text{O}_2]_{\text{ex}}$ , external hydrogen peroxide concentration;  $[\text{H}_2\text{O}_2]_{\text{in}}$ , intracellular (cytoplasmic)  $\text{H}_2\text{O}_2$  concentration arising from cell exposure to the external peroxide;  $\text{HyPer}_{\text{rd ss}}$ , steady-state level of the reduced HyPer fraction established with time due to the concurrent processes of sensor oxidation and reduction at different oxidative loads.

gradients established in oxidatively stressed human cells of different phenotypes. To ensure that our results would not depend on the individual characteristics of a donor, we chose for our experiments the set of cell lines that consists of human mesenchymal stem/stromal cells (MSCs) expressing HyPer in the cell cytoplasm, induced pluripotent stem cells (iPSCs) derived from MSCs using cell reprogramming method, and differentiated progenies of iPSCs with the phenotype resembling precursory MSCs (iPSC-MSCs). The percentage of iPSCs expressing the sensor remained the same, and in iPSC-MSCs decreased slightly compared to parental MSC cultures (91% against 94%) (Fig. 3). iPSCs possessed all canonical features of pluripotent cells, such as clonal growth morphology, expression of Oct-4, Sox-2, NANOG, SSEA-4, alkaline phosphatase, and the ability to differentiate into cell types of three germ layers (Fig. 4A). iPSC-MSCs meet all minimal criteria for defining multipotent mesenchymal stem/stromal cells formulated by the International Society for Cellular Therapy [18] – cells were characterized by fibroblast-like morphology, expression of mesodermal marker vimentin, MSC-specific surface markers (CD 90, CD 105, CD 44, CD73, CD 140b) (Fig. 4B), and ability to differentiate into osteoblasts and adipocytes (Supplemental Fig. S4). Apart from the lineages mentioned, we included in the comparison the cancer cell line HeLa that is widely used as a model system in redox biology studies.

For these cell lines, we repeated the experiments carried out on K-562 cells. The results partly resembled previously obtained data. In particular, the flow cytometer settings, adjusted earlier to perform normalization of HyPer signals (see Results, 3.1. Section), occurred to be suitable for all types of the cells. Besides, carrying out the calibration of HyPer signals, we found that the addition of DTT in the concentrations of up to 30 mM did not lead to the changes in HyPer fluorescence in any cell line, indicating a full reduction of HyPer in the cytoplasm of cells under normal conditions. In contrast, the reaction of cells to  $\text{H}_2\text{O}_2$ -induced stress varied between the assayed cell lines (Fig. 5 A, B). For example, a strong difference was observed in the amounts of external

$\text{H}_2\text{O}_2$  ensuring full sensor oxidation after the 10-min exposure (Fig. 5 B). 20  $\mu\text{M}$  of  $\text{H}_2\text{O}_2$  led to the full oxidation of HyPer only in K-562 cells, while 100  $\mu\text{M}$  oxidized the sensor almost completely in all types of the cells (Fig. 5 B). Correspondingly, to compare the potency of antioxidant defense in different cells both at low and high oxidative loads, we chose the 20–100  $\mu\text{M}$  range of external  $\text{H}_2\text{O}_2$  concentrations. To characterize these loads, we investigated their impact on cell viability after 24-h exposure to  $\text{H}_2\text{O}_2$  and found a significant difference between the oxidative stress responses in various types of the cells. For example, in some lines (ex: MSCs), 50  $\mu\text{M}$  concentration (2 pmol/cell) did not lead to the cell death (Fig. 5A) but caused DNA breaks (Supplemental Fig. S5). At the same time, in iPSC cultures, this dose caused the death of approximately 50% of the cells (Fig. 5A), and in K-562 cells, as we showed previously (Fig. 2C), it was absolutely lethal. Based on these findings, we classified the 20–100  $\mu\text{M}$  range of  $\text{H}_2\text{O}_2$  concentrations as cell-damaging under the experimental conditions used, at least in the case of long-term expositions.

Finally, for all cell lines used, we analyzed the kinetics of sensor oxidation during the first 10 min immediately after  $\text{H}_2\text{O}_2$  addition to cell suspensions and calculated the  $\text{H}_2\text{O}_2$  gradients in the 20–100  $\mu\text{M}$  range of extracellular concentrations (Fig. 5C and D). We found that the kinetics of HyPer oxidation was exponential in all cell types. Similar to K-562 cells, gradients of  $\text{H}_2\text{O}_2$  obtained from the kinetic measurements did not depend on extracellular  $\text{H}_2\text{O}_2$  concentration at high oxidative loads ( $> 50 \mu\text{M}$ ), being substantially lower than those at 20  $\mu\text{M}$  of  $\text{H}_2\text{O}_2$ . Interestingly, in normal human cells (MSCs, iPSCs, and iPSC-MSCs), the gradients were significantly higher than in cancer (K-562 and HeLa). The highest gradients (more than  $10^3$  under all loads tested), and, therefore, the most potent antioxidant defense, was found in iPSCs and iPSC-MSCs. In iPSCs, gradients occurred two times higher than that in their parental MSC cultures. Surprisingly, differentiation of iPSCs, which led to the restoration of mesenchymal phenotype, did not result in alterations in antioxidant defense capacity. The antioxidant activity in the

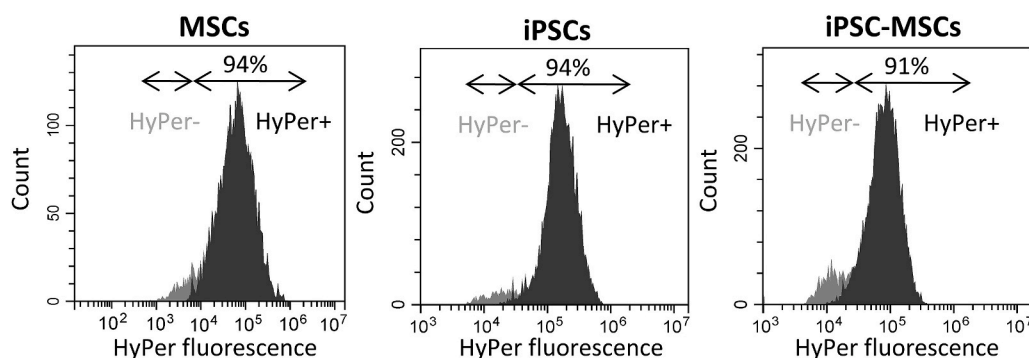


**Fig. 3. A percentage of HyPer-positive cells in different cell lines assayed.** Abbreviations: MSCs, human mesenchymal stem/stromal cells; iPSCs, induced pluripotent stem cells derived from MSCs by reprogramming; iPSC-MSCs, MSC-like differentiated progenies of iPSCs; HyPer-, HyPer-negative cell population; HyPer+, HyPer-positive cell population.

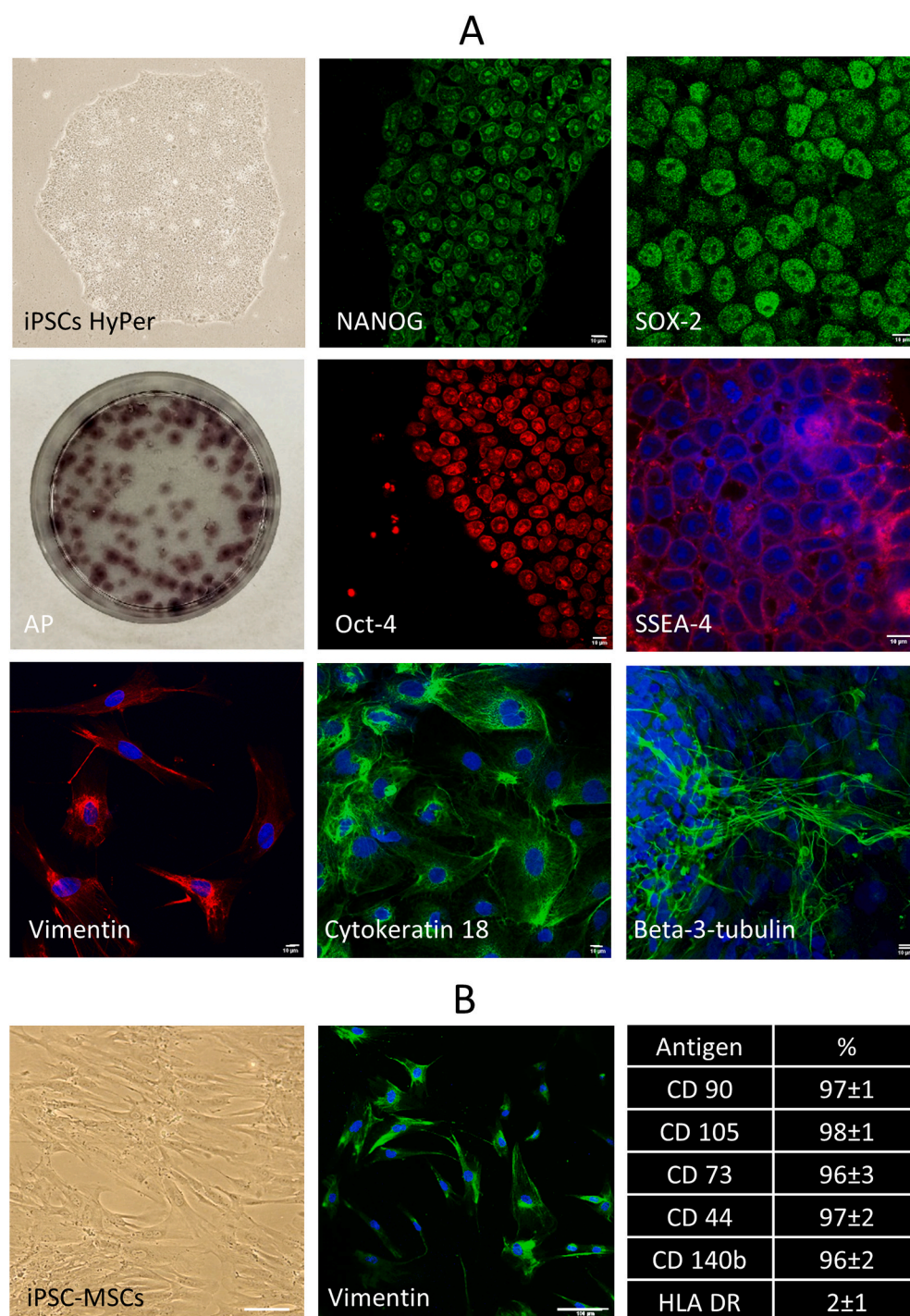


**Fig. 4. Characterization of iPSC and iPSC-MSC cultures. (A)** Morphology of iPSC clone and expression of pluripotent markers (1st and 2nd rows); the ability of iPSCs to differentiate into different cell types of three germ layers (3rd row), scale bar = 10  $\mu$ m. **(B)** Characterization of iPSC-MSC culture – cell morphology, expression of mesenchymal marker vimentin and MSC-specific surface markers, scale bar = 100  $\mu$ m. Abbreviations: MSCs, human mesenchymal stem/stromal cells; iPSCs, induced pluripotent stem cells derived from MSCs by reprogramming; iPSC-MSCs, MSC-like differentiated progenies of iPSCs; AP, alkaline phosphatase.

cytoplasm of progeny cells (iPSC-MSCs) was similar to that in their pluripotent parental cells and exceeded that of their MSC ancestors.

#### 4. Discussion

The high rate of redox reactions together with the limited number of analytical methods make it hard to implement the quantitative analysis of various intracellular redox parameters. In this study,  $H_2O_2$  biosensor HyPer was used as a reporter protein whose oxidation/reduction dynamics allows quantitative assessment of the redox activity in living cells. Analyzing the oxidation dynamics of HyPer sensor in the cytoplasm of the cells exposed to exogenous  $H_2O_2$ , we measured the gradient

that is established between the extracellular and cytoplasmic  $H_2O_2$  concentrations.

We found that in all human cell assayed the  $H_2O_2$  gradient depends on the oxidative loads on cells that perfectly fits with data, previously obtained in the experiments on yeast [10]. At low (<50  $\mu$ M)  $H_2O_2$  extracellular concentrations which resulted in the partial cytoplasmic sensor oxidation, the gradient decreased as oxidative loads increased. At high oxidative loads ensuring complete oxidation of HyPer, the gradient value stabilized. It is clear (see Eq. (2)) that the sensor can be fully oxidized only under the condition of  $k_{rd} = 0$ , i.e. at complete oxidation of thiol-disulfide exchange enzymes which are responsible for the HyPer redox-active domain reduction (presumably, thioredoxin system [10,22,



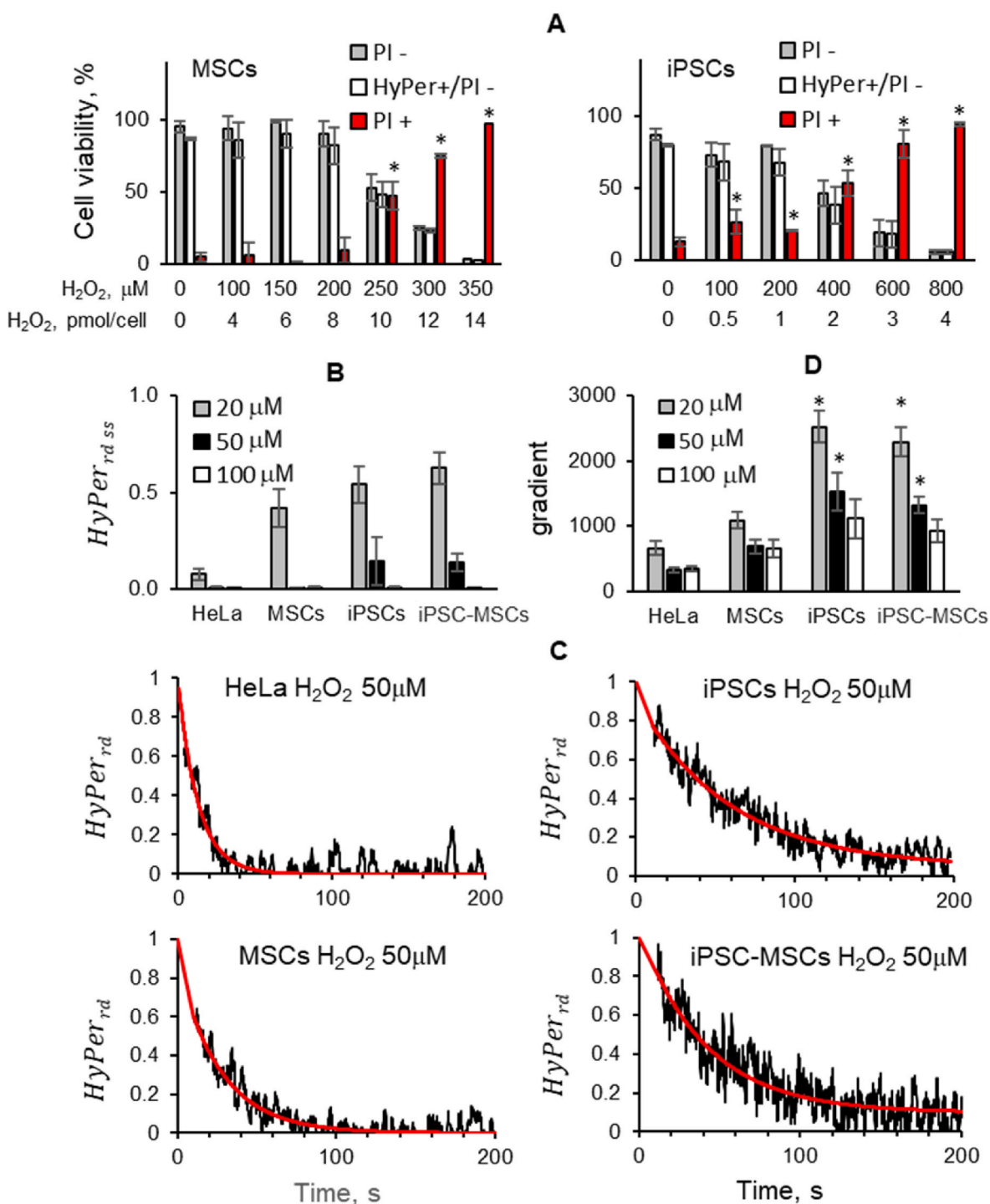


**Fig. 5.** Measurement of the peroxide gradient in human cells of different phenotypes upon exposure to different concentrations of  $\text{H}_2\text{O}_2$ . (A) Viability of MSCs and iPSCs after long-term exposure to different concentrations of  $\text{H}_2\text{O}_2$ : total (PI-) and HyPer-positive (HyPer+/PI-) populations of viable cells, as well as non-viable (PI+) cell fractions, revealed after 24-h exposure to different concentrations of  $\text{H}_2\text{O}_2$  (corresponding  $\text{H}_2\text{O}_2$  doses are shown below the axis). (B) Steady-state level of the reduced HyPer fraction established due to the concurrent processes of sensor oxidation and reduction at different oxidative loads in different cells. (C) Kinetics of the reduced HyPer fraction drop after  $\text{H}_2\text{O}_2$  (50  $\mu\text{M}$ ) addition to cell suspensions; curves were fitted (red lines) with Eq. (1) (Methods section), and  $\text{H}_2\text{O}_2$  gradient values (shown in D) were derived from these fits. (D) Gradients between the extracellular and cytoplasmic peroxide concentrations measured at different  $\text{H}_2\text{O}_2$  loads in different cell lines (calculated using Eqs. (1)–(7), Methods section). Data (A, B, D) are shown as mean  $\pm$  SD ( $N > 3$ ). Abbreviations: MSCs, human mesenchymal stem/stromal cells; iPSCs, induced pluripotent stem cells derived from MSCs by reprogramming; iPSC-MSCs, MSC-like differentiated progenies of iPSCs;  $\text{HyPer}_{rd}$ , reduced HyPer fraction;  $\text{HyPer}_{rdss}$ , the steady-state level of the reduced HyPer fraction; PI-, propidium iodide-negative (viable) cells; PI+, propidium iodide-positive (non-viable) cells; HyPer+/PI-, HyPer-positive viable cells. (For interpretation of the references to colour in this figure legend, the reader is referred to the Web version of this article.)



23]). Correspondingly, we suggested that it is the functional status of the thioredoxin-dependent enzymatic system that drives the dependence of the  $H_2O_2$  gradient on the oxidative load. To check this assumption, using the thioredoxin reductase inhibitor auranofin, we performed experiments on cells with diminished thioredoxin activity. In auranofin-treated cells, the values of the  $H_2O_2$  gradient perfectly matched those observed in the control cells at high oxidative loads. Thus, our data confirm the principal role of the thioredoxin-dependent enzymes (presumably, peroxiredoxins) in the processes of  $H_2O_2$  detoxification at low oxidative loads in human cells assayed. Importantly, it has been recently shown that the same enzymatic systems shape the intracellular  $H_2O_2$  gradients as well [27].

Measurements of  $H_2O_2$  gradients made it possible to characterize quantitatively the potency of the antioxidant defense system in human cells of different phenotypes – in cancer and normal cell lines. The gradient in cancer cell lines K-562 and HeLa measured at high oxidative loads amounted to several hundred times that fits well with theoretical and empirical estimates made previously [8,12]. At the same time, we revealed that this gradient can be significantly higher in normal cells, exceeding the value of  $10^3$ . When analyzing these data, we assumed that K-562 and HeLa cells, maintained in culture for a prolonged time, may differ significantly from cells of parental tumors due to their high adaptive capacity and plasticity. The latter can be the cause of the observed difference in gradients in comparison to normal human cells recently isolated from the donor tissues. Evidently, the method elaborated in this study can be used further to perform a more accurate comparison of redox systems of cancerous and normal human cells.

To overcome the problem of specificity of cell sources while comparing the antioxidant potency of cells with different phenotypes, we focused on isogenic human cell lines obtained using the cell reprogramming technique. MSCs expressing HyPer in the cell cytoplasm were reprogrammed to iPSCs. In the latter cells, the  $H_2O_2$  gradients were markedly increased in comparison to MSCs both at low and high oxidative loads that points to the enhancement of cell antioxidant defense upon reprogramming. To clarify whether the increased antioxidant activity in the cell cytoplasm is a characteristic feature of pluripotent cells, we differentiated iPSCs and measured the  $H_2O_2$  gradients in differentiated progeny cells (iPSC-MSCs). iPSC-MSCs exhibited a phenotype similar to the MSC ancestors, but, surprisingly, possessed much higher antioxidant activity, resembling that of parental iPSCs. This observation allows us to suggest that the intensification of the  $H_2O_2$ -detoxification process is not a characteristic feature of pluripotent phenotype but is rather related to a period of early human development.

When analyzing the ability of different cell cultures to resist  $H_2O_2$ -induced stress, it was important to investigate the impact of applied oxidative loads on cell physiology. For this purpose, we evaluated the viability of cells exposed to  $H_2O_2$ . It is known that under oxidative stress conditions, the damaging factor is not a concentration, but a dose of  $H_2O_2$  that is detoxified by a cell. Therefore we used long-term (24-h) incubations in the viability tests to achieve the total decomposition of the  $H_2O_2$  by cells, which enabled us to assess exactly the applied  $H_2O_2$  doses. Under such conditions and the cell density of 25,000 cells per 1 mL of the medium, the 20–100  $\mu M$  range of  $H_2O_2$  concentrations corresponded to the 0.8–4 pmole/cell range of  $H_2O_2$  doses. Cell viability tests showed that these doses were not cytotoxic to MSCs but yet led to the damage of cell DNA. Our previous studies [24,25] revealed that genotoxic stress induced in these cells by  $H_2O_2$  dose of 4 pmol/cell can result in premature cellular senescence. In contrast, in the case of iPSCs and K-562 cells, the doses in the range of 0.8–4 pmole/cell caused cytotoxic effects, at least in the part of cell population. In the experiments with K-562 cells we used the wider range of  $H_2O_2$  doses, and the lowest ones (<0.3 pmole/cell), which did not result in the thioredoxin system exhaustion, were not cytotoxic. Correspondingly, we classified the 20–100  $\mu M$  range of  $H_2O_2$  concentrations, which we used for the comparison of antioxidant activity in the different cell types, as damaging ones, associating this damage with the exhaustion of

thiol-disulfide capacity in cells observed under the high oxidative loads. Intriguingly, whether these loads are within or beyond the range that cells could see *in vivo*, still remains unclear. According to published data, the 20–100  $\mu M$  concentrations exceed the most probable normal values of plasma  $H_2O_2$  concentrations in humans (1–5  $\mu M$ ), and fall into the diapason which is probably related to certain disease states or chronic inflammation [26]. At the same time, the ratio of plasma volume in tissue capillaries to the mass of cells contacting with plasma is much lower than the ratio of media volume to the mass of cells in the suspensions we used. Therefore, we speculate that the doses of  $H_2O_2$  which cells detoxified during the 24-h incubations in our experiments (at least, at 20 and may be at 50  $\mu M$  concentrations) can be relevant to the situation of chronic oxidative stresses *in vivo*, when cells are exposed to plasma  $H_2O_2$  concentrations of tens of micromoles for quite a long time. Simultaneously, we suppose that the lowest concentrations (<20  $\mu M$ ), which we used in the experiments with K-562 cells, may have relevance to the normal cell physiology *in vivo*.

Apart from monitoring HyPer oxidation under the oxidative stress conditions, we have evaluated the basal level of HyPer oxidation in different cell types. We found that the cytoplasmic HyPer sensor is fully reduced in cells with normal metabolism suspended in a complete growth medium. These observations are consistent with the already published research [22] but differ from our previously obtained data related to K-562 cells suspended in PBS [12]. According to [12], HyPer is slightly oxidized (~10%) under such conditions. Our present findings suggest that this effect is probably due to the lack of nutrients in PBS. Perhaps, the full growth medium is needed to support the normal redox metabolism ensuring full reduction of the redox-active thiol groups of HyPer under basal conditions. Indeed, the value of  $H_2O_2$  gradient measured under low oxidative loads in K-562 cells suspended in PBS (~400 [12]) is very close to that measured in the present study at fully exhausted thioredoxin activity in the cell cytoplasm ( $440 \pm 20$ ).

Another question we raised is the impact of ectopic expression of HyPer on antioxidant system activity in cells under conditions of oxidative distress. To answer it, we compared the  $H_2O_2$  gradients in K-562 cells with low and high amounts of HyPer and found no differences in these values. Moreover, after administration of exogenous  $H_2O_2$ , the percentage of dead cells was equal in HyPer-positive and negative cells. In accordance with the previously published findings [10], the obtained results can be explained by the slow rate of HyPer redox-active domain reduction. Due to its slow reduction, HyPer cannot compete with the enzymes providing  $H_2O_2$  detoxification, and thus it cannot be considered as an antioxidant.

## 5. Conclusions

In this study, we investigated the potency of antioxidant defense in human cells of different phenotypes based on the quantitative evaluation of the gradient between the extracellular and cytoplasmic  $H_2O_2$  concentrations under the steady-state oxidative load. We show that at low oxidative loads the gradient depends on the extracellular  $H_2O_2$  concentration. At the same time, at high oxidative loads, which cause the full exhaustion of thioredoxin activity in the cell cytoplasm, the gradient stabilized, pointing out that it is the functional status of the thioredoxin-dependent enzymatic system that drives the dependence of the  $H_2O_2$  gradient on the oxidative load in human cells. We found that in widely used cancer cell lines (K-562 and HeLa) it amounts to hundreds of times. In normal human cells (MSCs, iPSCs derived from MSCs, and differentiated iPSC progenies with MSC-like phenotype) the gradient can exceed  $10^3$ . We found that the reprogramming of the cells causes the enhancement of their antioxidant potency, while subsequent differentiation of iPSCs does not necessarily lead to changes in the activity of antioxidant defense systems, assuming that intensification of the  $H_2O_2$ -detoxification process is inherent to a period of early human development. We suggest that the method elaborated in this study can be applied for further in-depth studies of redox activities in human cells.

## Declaration of competing interest

The authors have no conflict of interest.

## Acknowledgments

The authors acknowledge support from the Russian Science Foundation (Grant No. 21-74-20178). Experiments were performed using facilities of the shared research facility “Vertebrate cell culture collection” supported by the Ministry of Science and Higher Education of the Russian Federation (Agreement No. 075-15-2021-683).

## Appendix A. Supplementary data

Supplementary data to this article can be found online at <https://doi.org/10.1016/j.redox.2022.102245>.

## References

- [1] S.G. Rhee, Redox signaling: hydrogen peroxide as intracellular messenger, *Exp. Mol. Med.* 31 (1999) 53–59, <https://doi.org/10.1038/emm.1999.9>.
- [2] J.R. Stone, S. Yang, Hydrogen peroxide: a signaling messenger, *Antioxidants Redox Signal.* 8 (2006) 243–270, <https://doi.org/10.1089/ars.2006.8.243>.
- [3] H. Sies, Hydrogen peroxide as a central redox signaling molecule in physiological oxidative stress: oxidative eustress, *Redox Biol.* 11 (2017) 613, <https://doi.org/10.1016/j.redox.2016.12.035>.
- [4] H. Sies, C. Berndt, D.P. Jones, *Oxidative Stress* 86 (2017) 715–748, <https://doi.org/10.1146/Annurev-Biochem-061516-045037>.
- [5] H. Sies, *Biochemistry of oxidative stress*, *Angew Chem. Int. Ed. Engl.* 25 (1986) 1058–1071, <https://doi.org/10.1002/ANIE.198610581>.
- [6] F. Antunes, E. Cadenas, Estimation of H<sub>2</sub>O<sub>2</sub> gradients across biomembranes, *FEBS Lett.* 475 (2000), [https://doi.org/10.1016/S0014-5793\(00\)01638-0](https://doi.org/10.1016/S0014-5793(00)01638-0).
- [7] H.S. Marinho, L. Cyrne, E. Cadenas, F. Antunes, The cellular steady-state of H<sub>2</sub>O<sub>2</sub>: latency concepts and gradients, in: *Methods Enzymol.* 2013, <https://doi.org/10.1016/B978-0-12-405882-8.00001-5>.
- [8] B.K. Huang, H.D. Sikes, Quantifying intracellular hydrogen peroxide perturbations in terms of concentration, *Redox Biol.* 2 (2014), <https://doi.org/10.1016/j.redox.2014.08.001>.
- [9] J.B. Lim, T.F. Langford, B.K. Huang, W.M. Deen, H.D. Sikes, A reaction-diffusion model of cytosolic hydrogen peroxide, *Free Radic. Biol. Med.* 90 (2016), <https://doi.org/10.1016/j.freeradbiomed.2015.11.005>.
- [10] A. Domènech, J. Ayté, F. Antunes, E. Hidalgo, Using in vivo oxidation status of one- and two-component redox relays to determine H<sub>2</sub>O<sub>2</sub> levels linked to signaling and toxicity, *BMC Biol.* 16 (2018), <https://doi.org/10.1186/s12915-018-0523-6>.
- [11] A.V. Peskin, N. Dickerhof, R.A. Poynton, L.N. Paton, P.E. Pace, M.B. Hampton, C. C. Winterbourn, Hyperoxidation of peroxiredoxins 2 and 3: rate constants for the reactions of the sulfenic acid of the peroxidatic cysteine, *J. Biol. Chem.* 288 (2013) 14170–14177, <https://doi.org/10.1074/JBC.M113.460881>.
- [12] O. Lyublinskaya, F. Antunes, Measuring intracellular concentration of hydrogen peroxide with the use of genetically encoded H<sub>2</sub>O<sub>2</sub> biosensor HyPer, *Redox Biol.* 24 (2019) 101200, <https://doi.org/10.1016/j.redox.2019.101200>.
- [13] V.V. Belousov, A.F. Fradkov, K.A. Lukyanov, D.B. Staroverov, K.S. Shakhbazov, A. V. Terskikh, S. Lukyanov, Genetically encoded fluorescent indicator for intracellular hydrogen peroxide, *Nat. Methods* 3 (2006), <https://doi.org/10.1038/nmeth866>.
- [14] M. Zheng, F. Åslund, G. Storz, Activation of the OxyR transcription factor by reversible disulfide bond formation, *Science* 80 (1998) 279, <https://doi.org/10.1126/science.279.5357.1718>.
- [15] D.S. Bilan, V.V. Belousov, HyPer family probes: state of the art, *Antioxidants Redox Signal.* 24 (2016) 731–751, <https://doi.org/10.1089/ars.2015.6586>.
- [16] O.G. Lyublinskaya, S.A. Antonov, S.G. Gorokhovtsev, N.A. Pugovkina, J. S. Kornienko, J.S. Ivanova, A.N. Shatrova, N.D. Aksenov, V.V. Zenin, N. N. Nikolsky, Free radical biology and medicine flow cytometric HyPer-based assay for hydrogen peroxide, *Free Radic. Biol. Med.* 128 (2018) 40–49, <https://doi.org/10.1016/j.freeradbiomed.2018.05.091>.
- [17] V.I. Zemelko, T.M. Grinchuk, A.P. Domnina, I.V. Artzibasheva, V.V. Zenin, A. A. Kirsanov, N.K. Bichevaia, V.S. Korsak, N.N. Nikolsky, Multipotent mesenchymal stem cells of desquamated endometrium: isolation, characterization and use as feeder layer for maintenance of human embryonic stem cell lines, *Tsitologiya* 53 (2011) 919–929, <https://doi.org/10.1134/S1990519X12010129>.
- [18] M. Dominici, K. Le Blanc, I. Mueller, I. Slaper-Cortenbach, F. Marini, D. Krause, R. Deans, A. Keating, D. Prockop, E. Horwitz, Minimal criteria for defining multipotent mesenchymal stromal cells, in: *The International Society for Cell Biology* vol. 8, 2006, pp. 315–317, <https://doi.org/10.1080/14653240600855905>. M., Le Blanc, K., Mueller, I., Slaper-Cortenbach, I., Marini, F., Krause, D., ... Horwitz, E. (2006). Minimal criteria for defining multipotent mesenchymal stem cells, *Cytotherapy*.
- [19] C.M. Doskey, T.J. Van 'T Erve, B.A. Wagner, G.R. Buettner, Moles of a substance per cell is a highly informative dosing metric in cell culture, *PLoS One* 10 (2015), <https://doi.org/10.1371/journal.pone.0132572>.
- [20] P.M. Brito, F. Antunes, Estimation of kinetic parameters related to biochemical interactions between hydrogen peroxide and signal transduction proteins, *Front. Chem.* 2 (2014), <https://doi.org/10.3389/fchem.2014.00082>.
- [21] D.S. Bilan, L. Pase, L. Joosen, A.Y. Gorokhovtsev, Y.G. Ermakova, T.W.J. Gadella, C. Grabher, C. Schultz, S. Lukyanov, V.V. Belousov, HyPer-3: a genetically encoded H<sub>2</sub>O<sub>2</sub> probe with improved performance for ratiometric and fluorescence lifetime imaging, *ACS Chem. Biol.* 8 (2013), <https://doi.org/10.1021/cb300625g>.
- [22] L. de Cubas, V.V. Pak, V.V. Belousov, J. Ayté, E. Hidalgo, The mitochondria-to-cytosol h<sub>2</sub>o<sub>2</sub> gradient is caused by peroxiredoxin-dependent cytosolic scavenging, *Antioxidants* 10 (2021), <https://doi.org/10.3390/antiox10050731>.
- [23] P. Kritsiligkou, T.K. Shen, T.P. Dick, A comparison of Prx- and OxyR-based H<sub>2</sub>O<sub>2</sub> probes expressed in *S. cerevisiae*, *J. Biol. Chem.* 297 (2021), <https://doi.org/10.1016/j.jbc.2021.100866>. ATTACHMENT/F5E0786A-9A0E-4D35-8EF4-B563D2035099/MMC1.PDF.
- [24] E. Burova, A. Borodkina, A. Shatrova, N. Nikolsky, Sublethal oxidative stress induces the premature senescence of human mesenchymal stem cells derived from endometrium, *Oxid. Med. Cell. Longev.* 2013 (2013), <https://doi.org/10.1155/2013/474931>. Article ID 474931.
- [25] A. Borodkina, A. Shatrova, P. Abushik, N. Nikolsky, E. Burova, Interaction between ROS dependent DNA damage, mitochondria and p38 MAPK underlies senescence of human adult stem cells, *Aging (Albany, NY)* 6 (2014) 481–495, <https://doi.org/10.18632/aging.100673>.
- [26] H.J. Forman, A. Bernardo, K.J. Davies, What is the concentration of hydrogen peroxide in blood and plasma? *Arch. Biochem. Biophys.* 603 (2016) 48–53, <https://doi.org/10.1016/j.abb.2016.05.005>.
- [27] N. Mishina, Y. Bogdanova, Y. Ermakova, A. Panova, D. Kotova, D. Bilan, B. Steinhorn, E. Arnér, T. Michel, V. Belousov, Which Antioxidant System Shapes Intracellular H<sub>2</sub>O<sub>2</sub> Gradients, *Antioxid Redox Signal.* 31 (9) (2019) 664–670.